

# Translation and Rotation Invariant Histogram Features for Series of Images

Ana Pérez Grassi, Fernando Puente León

Fachgebiet Verteilte Messsysteme, Technische Universität München, 80290 München  
{a.perez, f.puente}@tum.de

**Abstract:** Some surfaces, like metallic and varnished ones, can only be properly controlled, if they are inspected under different illumination directions. This requires a three-dimensional input signal: a series of images, where each image shows the same surface but is illuminated from a different angle. This paper presents a method to extract translation and rotation invariant features from such a series to detect and classify topographic irregularities on the inspected surfaces. Invariant features are represented by 3D fuzzy histograms and classified by a support vector machine (SVM). The proposed method performs successfully on varnished wooden surfaces to detect and classify defects on the varnish film. This sort of defects is extremely difficult to recognize, which makes it appropriate to demonstrate the robustness of the method.

## 1 Introduction

Topographic irregularities on certain surfaces, e.g. metallic and varnished ones, can only be reliably recognized, if the corresponding surface is inspected under different illumination directions. Therefore, their automated inspection requires to record an image series in which each picture is taken under a different illumination angle. It is advantageous to analyze the series as a whole and not as a set of individual pictures, because the relevant information is contained not only in each picture but also in the relations among them. Consequently, the image series constitutes a 3D signal, and the extraction of features for the analysis should not be performed considering its dimensions as unconnected.

The presented approach is based on the local binary pattern (LBP) of Ojala et al. [OPM02] and on the method of Schael [Sch05] to detect and classify defects on textiles. These works classify textures and defects using invariant features, but considering only single images as input. In this paper, we propose a combination and extension of these methods to support series of images. A kernel function collects information within a local 3D neighborhood and fuses it to obtain a 2D result. The properties of invariant features are combined with those of histograms to achieve a higher discrimination power [SB98]. Finally, we test our method on varnished wooden surfaces to detect and classify defects on the varnish film.

The paper is organized as follows: Section 2 introduces the concept of invariance, in Section 3 we present our approach to construct invariant features from series of images, whereas Section 4 shows the results obtained with varnished wooden surfaces.

## 2 Invariant features

For a recognition task, different patterns of a group are considered equivalent if they convey to each other through an induced transformation. A feature is called invariant if, for a given transformation, it remains constant for all equivalent patterns [Sch95].

Let  $g(\mathbf{x})$  with  $\mathbf{x} = (x, y)^T \in \mathbb{R}^2$  denote a gray-scale image and  $\mathbf{m} = (m_1, \dots, m_d)^T$  a  $d$ -dimensional vector of invariant features, being  $m_l$  its  $l$ -th element. A common approach to construct a feature  $m_l$  out of  $g(\mathbf{x})$  that is invariant against a certain transformation group  $\mathcal{T}$  is integrating over this group [Hur97]:

$$m_l = \int_{\mathcal{T}} f_l(t\{g(\mathbf{x})\}) dt = \int_{\mathcal{P}} f_l(t(\mathbf{p})\{g(\mathbf{x})\}) d\mathbf{p}. \quad (1)$$

Equation (1) is known as the Haar integral, where  $f_l$  is an arbitrary, local kernel function,  $t \in \mathcal{T}$  is a transformation parametrized by the vector  $\mathbf{p} \in \mathcal{P}$ , and  $\mathcal{P}$  denotes the parameter space.

In this work, we aim at extracting invariant features with respect to the 2D Euclidean motion, which constitutes a finite and compact transformation group composed of rotation and translation in  $\mathbb{R}^2$ . Then, the parameter vector is given as follows:  $\mathbf{p} = (\tau_x, \tau_y, \varphi)^T$ , where  $\tau_x$  and  $\tau_y$  denote the translation parameters in  $x$  and  $y$  direction, and  $\varphi$  is the rotation parameter. The compactness and finiteness of this group guarantee the convergence of the integral [Sch95]. For this group, Eq. (1) can be rewritten as:

$$m_l = \int_{\mathcal{P}} f_l(t(\tau_x, \tau_y, \varphi)\{g(\mathbf{x})\}) d\tau_x d\tau_y d\varphi. \quad (2)$$

## 3 Invariant features for series of images

In this paper, the input function is not a single image but a series obtained by systematically varying the illumination angle [LP06]. The series of images can be referred to as  $g(\mathbf{x}; \omega)$ , where  $\omega \in [0, 2\pi)$  is a cyclic parameter that indicates the illumination azimuth used for image acquisition, and consequently the picture location within the series. Since series of images are discontinuous along  $\omega$ , it is sensible to define  $\omega$  as a discrete parameter:

$$\omega_b = b \Delta\omega \quad \text{with} \quad 0 \leq b \leq B-1, \quad B = \frac{2\pi}{\Delta\omega},$$

where  $B$  denotes the number of pictures in the series. Let us reshape Eq. (2) to consider series of images:

$$m_l = \int_{\mathcal{P}} f_l(t(\tau_x, \tau_y, \varphi)\{g(\mathbf{x}; \omega_b)\}) d\tau_x d\tau_y d\varphi.$$

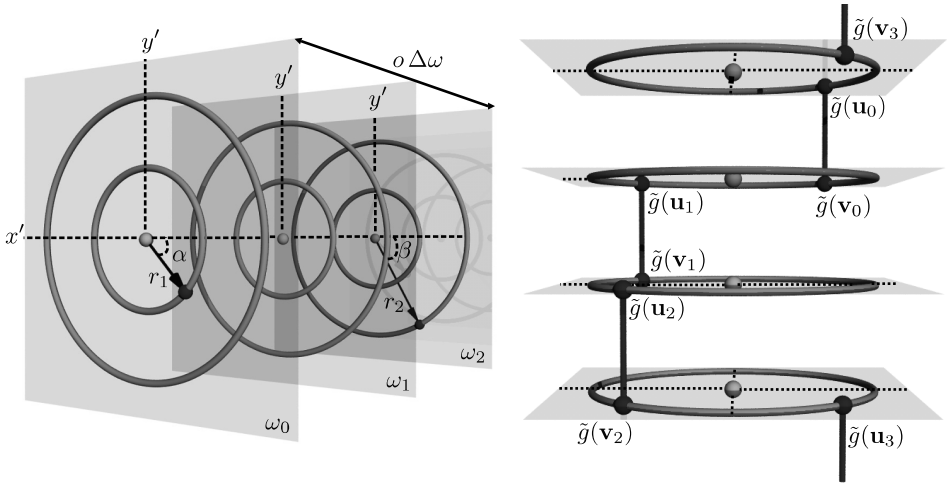


Figure 1: Left: Parameters of the kernel function. In this example,  $o = 2$  holds. Right: Schematic representation of  $f_l$  for  $r_1 = r_2$ ,  $o = 1$ ,  $\alpha = \beta = 45^\circ$  and an image series with  $B = 4$ . The connected pairs of points  $\tilde{g}(\mathbf{u}_b)$  and  $\tilde{g}(\mathbf{v}_b)$  represent the subtrahends of  $f_l$  for different values of  $b$ .

In this case, the transformed series  $t(\tau_x, \tau_y, \varphi)\{g(\mathbf{x}; \omega_b)\}$  can be expressed as follows:

$$t(\tau_x, \tau_y, \varphi)\{g(\mathbf{x}; \omega_b)\} =: \tilde{g}(\mathbf{x}'; \omega_b) \quad \text{with} \quad \mathbf{x}' = \begin{pmatrix} \cos \varphi & \sin \varphi \\ -\sin \varphi & \cos \varphi \end{pmatrix} \mathbf{x} - \begin{pmatrix} \tau_x \\ \tau_y \end{pmatrix}.$$

### 3.1 Kernel function

The proposed kernel function  $f_l$  operates on a 3D neighborhood and presents a circular symmetry along  $b$ . This local function is defined as follows:

$$\begin{aligned} f_l(\mathbf{p}) &= \frac{1}{B} \sum_{b=0}^{B-1} |\tilde{g}(\mathbf{u}_b) - \tilde{g}(\mathbf{v}_b)|, \\ \mathbf{u}_b &= \left( \begin{bmatrix} r_{1,l} \cos(\alpha_l + \omega_b) \\ -r_{1,l} \sin(\alpha_l + \omega_b) \end{bmatrix}; \omega_b \right), \\ \mathbf{v}_b &= \left( \begin{bmatrix} r_{2,l} \cos(\beta_l + \omega_b) \\ -r_{2,l} \sin(\beta_l + \omega_b) \end{bmatrix}; (\omega_b + o \Delta \omega) \bmod 2\pi \right). \end{aligned} \quad (3)$$

The meaning of the parameters  $r_1$ ,  $r_2$ ,  $\alpha$ ,  $\beta$ , and  $o$  is illustrated on left side of Fig. 1. The right side of the figure shows the local configuration of the pixels compared by the kernel function  $f_l$  schematically.

### 3.2 Histogram features

With Eq. (3), invariant features can be constructed by integrating over the group of transformations parametrized by the vector  $\mathbf{p}$ , as stated in Section 2:

$$m_l = \int_{\mathcal{P}} f_l(\mathbf{p}) d\mathbf{p}.$$

An alternative way to achieve invariance is not to perform an integration, but to compute a histogram. This leads to features with more discriminative power and the same invariance properties [SB98]. The construction of histograms requires the use of discrete parameters:

$$g_{mnb} := g(\mathbf{x}; \omega_b) \quad \text{with} \quad x = m \Delta x, \quad y = n \Delta y,$$

$$0 \leq m \leq M-1, \quad 0 \leq n \leq N-1,$$

$$\mathbf{p}_{ijk} := (i \Delta x, j \Delta y, k \Delta \varphi), \quad 0 \leq k \leq K-1, \quad K = \frac{2\pi}{\Delta \varphi}.$$

To this end, we define a 3D matrix  $\mathbf{H}$  of size  $M \times N \times K$  with the following elements:

$$h_{ijk} := f_l(\mathbf{p}) = f_l(i \Delta x, j \Delta y, k \Delta \varphi).$$

To achieve invariance against rotation, each of the  $K$ -tuples of the matrix  $\mathbf{H}$  resulting for arbitrary locations  $(i, j)$  must be sorted in ascending order along the corresponding  $k$  dimension. This results in a sorted matrix  $\mathbf{H}^*$ , whose elements are referred to as follows:

$$h_{ijk}^* := h_{ij(k)}.$$

Following, for each  $k \in \{0 \dots, K-1\}$  a 2D matrix  $\mathbf{H}'_k$  with elements  $(h'_k)_{ij} := h_{ijk}^*$  is extracted from the matrix  $\mathbf{H}^*$ , and a fuzzy histogram is constructed from each  $\mathbf{H}'_k$ . Fuzzy histograms overcome the problem of an unsteady assignment at bin boundaries presented by classical histograms [SB98]. The resulting  $k$  histograms are associated forming a 3D histogram, which constitutes a translation and rotation invariant descriptor.

Large changes in the pixel intensities along the third dimension  $b$  of the series can indicate topographic defects on the surface. However, defects are in general small compared with the inspected surface. Consequently, the number of pixels with intensities varying strongly along  $b$  is very low compared with those that present almost no change. For this reason, most information is concentrated in the first histogram's bins, whereas the remaining bins feature almost no weight within the classification process. Two modifications are introduced to improve this situation. Firstly, a logarithmic function is incorporated to  $f_l$ . Secondly, the bins are weighted by an exponential function  $Q^c$ , where  $Q$  is a constant, and  $c$  denotes the corresponding bin number. The logarithm decompresses the information of the first bins, and the weighting function raises the influence of the last ones:

$$f'_l(\mathbf{p}) = \frac{1}{B} \sum_{b=0}^{B-1} \log_2 |\tilde{g}(\mathbf{u}_b) - \tilde{g}(\mathbf{v}_b) + 1|.$$

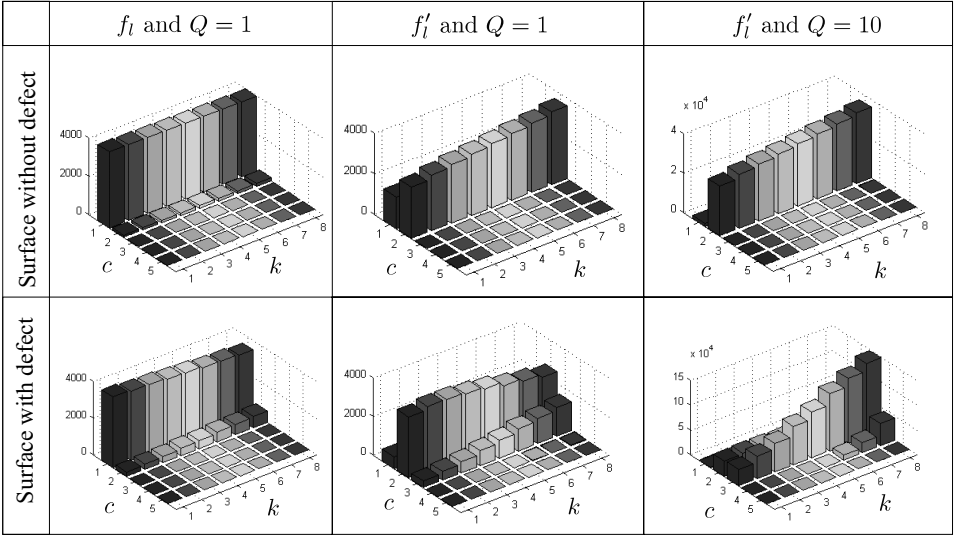


Figure 2: Histogram modifications for simulated surfaces with and without defect.

Figure 2 shows the effect introduced by these modifications in the histograms for simulated surfaces with as well as without defects. It is clearly visible that each modification increases the difference between the features of both classes (defective and non-defective), improving thus their separability.

## 4 Results

The presented method has been tested on varnished wooden surfaces to detect defects on the varnish film. All samples have a transparent varnish film and the wood texture is also visible. Defects on the varnish film are only partially visible under certain illumination conditions. Additionally, the texture of the underlying surface constitutes a noisy background which may mask out some defects. All these characteristics increase the complexity of the surfaces under analysis for an automated inspection [PAP06].

For each surface,  $B = 8$  pictures have been taken by varying the illumination azimuth in steps of  $45^\circ$ . The invariant features have been computed in windows of 16 by 16 pixels. Four different classes of defects have been considered: fissures, craters, bubbles, and blisters. A SVM has been used for the classification, for which the learning process has been performed based on a training list consisting of 20 series of images showing different defects on different wood substrates. Five different histograms were extracted using different combinations of the parameters  $r_1$ ,  $r_2$ ,  $\alpha$ ,  $\beta$ , and  $o$ .

The proposed set of features reliably describes the relevant information contained in the image series and enables a correct detection and classification of the defects. The method

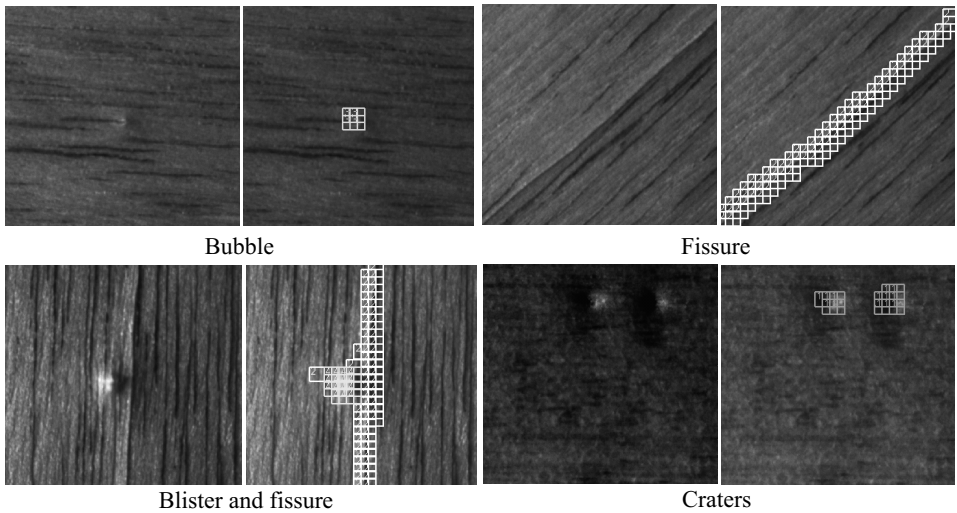


Figure 3: Results: (left) image of the series; (right) classification results.

behaves robustly and is able to detect and classify defects on different wood textures. Figure 3 shows some results, where the five different classes of regions (all four types of defects as well as non-defective areas) could all be correctly classified.

## References

- [Hur97] A. Hurwitz. Über die Erzeugung der Invarianten durch Integration. *Nachr. Akad. Wiss. Göttingen*, 1897.
- [LP06] C. Lindner and F. Puente León. Segmentierung strukturierter Oberflächen mittels variabler Beleuchtung. *Technisches Messen*, 73(4):200–207, 2006.
- [OPM02] T. Ojala, M. Pietikäinen, and T. Mäenpää. Multiresolution gray-scale and rotation invariant texture classification with local binary patterns. *IEEE Transactions on Pattern Analysis and Machine Intelligence*, 24(7), July 2002.
- [PAP06] A. Pérez Grassi, M.A. Abián Pérez, F. Puente León, and R.M. Pérez Campos. Detection of circular defects on varnished or painted surfaces by image fusion. In *Proceedings of the IEEE International Conference on Multisensor Fusion and Integration for Intelligent Systems*, pages 255–260, Heidelberg, 3–6 September 2006.
- [SB98] S. Siggelkow and H. Burkhardt. Invariant feature histograms for texture classification. In *Proceedings of the 1998 Joint Conference on Information Sciences (JCIS'98)*, North Carolina, USA, October 1998.
- [Sch05] Marc Schael. *Methoden zur Konstruktion invarianter Merkmale für die Texturanalyse*. PhD thesis, Albert-Ludwigs-Universität Freiburg, 2005.
- [Sch95] Hanns Schulz-Mirbach. *Anwendung von Invarianzprinzipien zur Merkmalgewinnung in der Mustererkennung*. PhD thesis, Technische Universität Hamburg-Harburg, 1995.